FINITE ELEMENT METHODS FOR MAXWELL EQUATIONS

LONG CHEN

First, we present two finite element spaces for Maxwell's equations, discuss the interpolation error. We then provide a convergence analysis for finite element methods using these spaces. We also give an introductory overview of finite element exterior calculus.

1. Finite Element Spaces

1.1. **Edge Elements.** We describe two types of edge elements developed by Nédélec [5, 6] in the 1980s. We recommend the readers to do the project *Project: Edge Finite Element Method for Maxwell-type Equations*.

1.1.1. *First family: the lowest order.* For the k-th edge $\boldsymbol{e}_k$ with vertices (i, j) and the direction from i to j, the basis $\boldsymbol{\phi}_k$ and corresponding degree of freedom $l_k(\cdot)$ are

$$\boldsymbol{\phi}_k = \lambda_i \nabla \lambda_j - \lambda_j \nabla \lambda_i,$$
$$l_k(\boldsymbol{v}) = \int_{e_k} \boldsymbol{v} \cdot \boldsymbol{t} \, \mathrm{d}s \approx \frac{1}{2}[\boldsymbol{v}(i) + \boldsymbol{v}(j)] \cdot \boldsymbol{e}_k,$$

where $\boldsymbol{t}$ is the unit tangent vector and the quadrature will be exact when $\boldsymbol{v} \cdot \boldsymbol{t}$ is linear.

We verify the duality $l_k(\boldsymbol{\phi}_k) = 1$ as follows

$$\boldsymbol{\phi}_k(i) \cdot \boldsymbol{e}_k = \nabla \lambda_j \cdot \boldsymbol{e}_k = \int_{e_k} \nabla \lambda_j \cdot \boldsymbol{t} \, \mathrm{d}s = \lambda_j(j) - \lambda_j(i) = 1$$
$$\boldsymbol{\phi}_k(j) \cdot \boldsymbol{e}_k = \nabla \lambda_i \cdot \boldsymbol{e}_k = \int_{e_k} \nabla \lambda_i \cdot \boldsymbol{t} \, \mathrm{d}s = \lambda_i(j) - \lambda_i(i) = -1,$$

and consequently $l_k(\boldsymbol{\phi}_k) = 1$. Consider the integral along another edge (m, n). If $(m, n) \cap (i, j) = \varnothing$, then $\lambda_i \mid_{e_{mn}} = \lambda_j \mid_{e_{mn}} = 0$. Without loss of generality, consider $m = i$ and $n \notin \{i, j\}$. Then in the basis $\boldsymbol{\phi}_k$ either $\nabla \lambda_j \cdot \boldsymbol{t}_{mn} = 0$ or $\lambda_j|_{e_{mn}} = 0$ and therefore $\boldsymbol{\phi}_k \cdot \boldsymbol{t}_{mn} = 0$. This verifies $l_\ell(\boldsymbol{\phi}_k) = 0$ for $\ell \neq k$.

In a tetrahedron T, the lowest order edge element is given by

$$\mathrm{NE}_0(T) = \mathrm{span}\{\boldsymbol{\phi}_k, k = 1, 2, \ldots, 6\}$$

which is a linear polynomial. We illustrate three basis functions associated with three edges on one face of the tetrahedron in Figure 2. Note that the vector field $\boldsymbol{\phi}_k$ for edge k is orthogonal to the other edges. For a 2D triangle, the formula for the basis is identical, and the three basis functions on a triangle are depicted in Figure 1.

The lowest order element $\mathrm{NE}_0(T)$ is merely a subspace of $\mathcal{P}_1^3$, which has a dimension of $4 \times 3 = 12$. In other words, the lowest order edge element represents an incomplete linear polynomial space and is capable of only reproducing a constant vector field. From an approximation standpoint, the L^2 error can only achieve a first-order accuracy. However, the $H(\mathrm{curl})$ norm of the error is also of the first order.

Date: Created: Spring 2014. Last update: May 14, 2024.

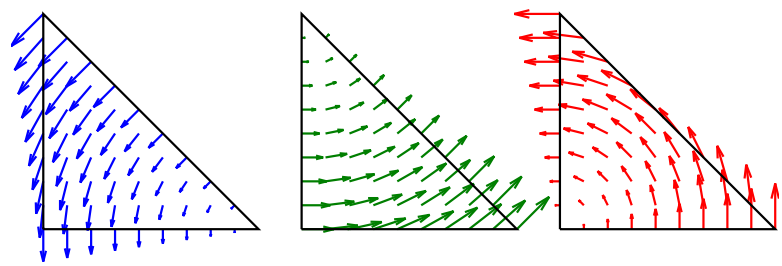

FIGURE 1. Three basis functions of NE_0 in a triangle.

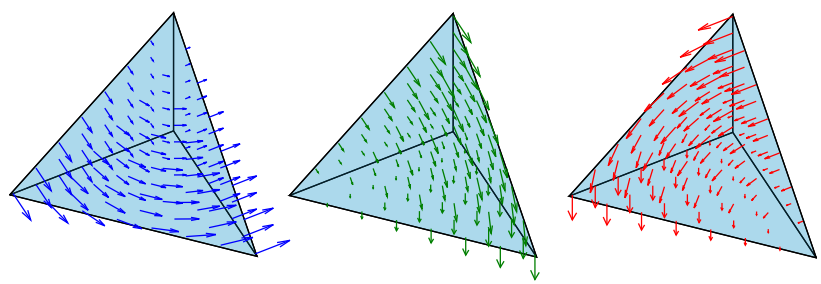

FIGURE 2. Three basis functions of NE_0 associated to three edges in a tetrahedron.

1.1.2. *Second family: the linear polynomial.* In addition to $\boldsymbol{\phi}_k$, for each edge, we introduce one more basis:

$$\boldsymbol{\psi}_k = \lambda_i \nabla \lambda_j + \lambda_j \nabla \lambda_i,$$
$$l_k^1(\boldsymbol{v}) = 3 \int_{e_k} \boldsymbol{v} \cdot \boldsymbol{t} (\lambda_i - \lambda_j) \, \mathrm{d}s \approx \frac{1}{2} [\boldsymbol{v}(i) - \boldsymbol{v}(j)] \cdot \boldsymbol{e}_k.$$

The quadrature is derived using Simpson's rule, taking into account the fact that $\lambda_i - \lambda_j = 0$ at the midpoint, which ensures exactness when $\boldsymbol{v} \cdot \boldsymbol{t}$ is linear. It is clear that $\{l_k(\cdot), l_k^1(\cdot), k = 1, 2, \ldots, 6\}$ are linearly independent. We then demonstrate that this set is dual to $\{\boldsymbol{\phi}_k, \boldsymbol{\psi}_k\}$. The Simpson's rule is exact for $l_k^1(\boldsymbol{\psi}_k)$ and thus

$$l_k^1(\boldsymbol{\psi}_k) = \frac{1}{2} [\boldsymbol{\psi}_k \cdot \boldsymbol{e}_{ij}(i) - \boldsymbol{\psi}_k \cdot \boldsymbol{e}_{ij}(j)] = \frac{1}{2} [(\lambda_i - \lambda_j)(i) - (\lambda_i - \lambda_j)(j)] = 1.$$

The verification of $\boldsymbol{\psi}_k \cdot \boldsymbol{e}_l = 0$, for $l \neq k$, is similar as before. Therefore $\{l_k^1\}$ is a dual basis of $\{\boldsymbol{\psi}_k\}$.

We also need to verify the duality conditions:

$$l_k(\boldsymbol{\psi}_l) = 0, \quad l_k^1(\boldsymbol{\phi}_l) = 0, \quad \forall l = 1, 2, \ldots, 6.$$

We only need to consider the case where $l = k$ since $\boldsymbol{\psi}_k \cdot \boldsymbol{t}_l = \boldsymbol{\phi}_k \cdot \boldsymbol{t}_l = 0$ for $l \neq k$. Note that $\boldsymbol{\psi}_k \cdot \boldsymbol{t}_k$ is an odd function (with respect to the midpoint), and thus its integral over the edge is zero. Similarly, $\boldsymbol{\phi}_k \cdot \boldsymbol{t}_k = 1$, which implies $l_k^1(\boldsymbol{\phi}_k) = 0$.

The lowest order second family of edge elements is defined as

$$\mathrm{NE}_1(T) = \mathrm{span}\{\boldsymbol{\phi}_k, \boldsymbol{\psi}_k, k = 1, 2, \ldots, 6\},$$

which forms a complete linear polynomial space capable of reproducing linear polynomials. As a result, the L^2-norm of the error is second-order. However, the $H(\mathrm{curl})$ norm

remains first-order, since $\boldsymbol{\psi}_k = \nabla(\lambda_i\lambda_j)$ and $\nabla \times \boldsymbol{\psi}_k = 0$ does not contribute to the approximation of the curl. The plot of $\boldsymbol{\psi}_k$ within a triangle is depicted in Figure 3.

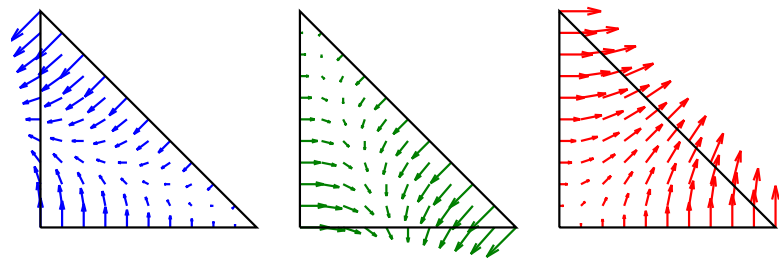

FIGURE 3. Basis vectors $\boldsymbol{\psi}_k$ of NE_1 in a triangle.

The global finite element space is obtained by gluing piecewise one. Using the barycentric coordinate in each tetrahedron, for an edge, the basis $\boldsymbol{\phi}_k, \boldsymbol{\psi}_k$ can be extend to all tetrahedron surrounding this edge. Given a triangulation $\mathcal{T}_h$, let $\mathcal{E}_h$ be the edge set of $\mathcal{T}_h$. Define

$$\begin{aligned}
\mathrm{NE}_0(\mathcal{T}_h) &= \mathrm{span}\{\boldsymbol{\phi}_e, e \in \mathcal{E}_h\} \\
&= \{\boldsymbol{v} \in L^2(\Omega), \boldsymbol{v}\,|_T \in \mathrm{NE}_0(T), \forall T \in \mathcal{T}_h,\ \ell_e(\boldsymbol{v}) \text{ is single valued } \forall e \in \mathcal{E}_h\}, \\
\mathrm{NE}_1(\mathcal{T}_h) &= \mathrm{span}\{\boldsymbol{\phi}_e, \boldsymbol{\psi}_e, e \in \mathcal{E}_h\} \\
&= \{\boldsymbol{v} \in L^2(\Omega), \boldsymbol{v}\,|_T \in \mathrm{NE}_1(T), \forall T \in \mathcal{T}_h,\ \ell_e(\boldsymbol{v}), \ell_e^1(\boldsymbol{v}) \text{ is single valued } \forall e \in \mathcal{E}_h\}.
\end{aligned}$$

To demonstrate that the obtained spaces indeed belong to $H(\mathrm{curl};\Omega)$, it is sufficient to verify the tangential continuity of the piecewise polynomials. Given a triangular face f, within a tetrahedron, we label the vertex opposite to f as x_f, and the corresponding barycentric coordinate will be denoted by λ_f. For an edge e that uses x_f as a vertex, the corresponding basis $\boldsymbol{\phi}_e$ or $\boldsymbol{\psi}_e$ is a linear combination of $\lambda_i\nabla\lambda_f$ and $\lambda_f\nabla\lambda_i$. When restricted to f, $\lambda_f\,|_f = 0$ and $\nabla\lambda_f \times \boldsymbol{n}_f = 0$ since $\nabla\lambda_f$ is a normal vector to f. Therefore, we have shown that $\boldsymbol{\phi}_e|_f \times \boldsymbol{n}_f = \boldsymbol{\psi}_e|_f \times \boldsymbol{n}_f = 0$ for edges e containing $\boldsymbol{n}_f$. Consequently, for $\boldsymbol{v} \in \mathrm{NE}_0(\mathcal{T}_h)$ or $\mathrm{NE}_1(\mathcal{T}_h)$, the trace $\boldsymbol{v}|_f \times \boldsymbol{n}_f$ depends solely on the basis functions of the edges of f, which is the desired tangential continuity for an $H(\mathrm{curl};\Omega)$ function.

We introduce the canonical interpolation into the edge element space. Define $I_h^{\mathrm{curl}} : V \cap \mathrm{dom}(I_h^{\mathrm{curl}}) \to \mathrm{NE}_0(\mathcal{T}_h)$ as follows: for a given function $\boldsymbol{u} \in V$, define $\boldsymbol{u}_I = I_h^{\mathrm{curl}}\boldsymbol{u} \in \mathrm{NE}_0(\mathcal{T}_h)$ by matching the degrees of freedom (d.o.f.):

$$l_e(I_h^{\mathrm{curl}}\boldsymbol{u}) = l_e(\boldsymbol{u}) \quad \forall e \in \mathcal{E}_h(\mathcal{T}_h).$$

That is,

$$\boldsymbol{u}_I = \sum_{e \in \mathcal{E}_h} \left(\int_e \boldsymbol{u} \cdot \boldsymbol{t}\, \mathrm{d}s \right) \boldsymbol{\phi}_e.$$

For the second family edge element space, include $l_e^1(\cdot)$ and $\boldsymbol{\psi}_e$ in the interpolation process.

Exercise 1.1. In one tetrahedron τ, verify I_h^{curl} to $\mathrm{NE}_0(\tau)$ will preserve constant vector and linear vectors for space $\mathrm{NE}_1(\tau)$.

To analyze the error $\nabla \times (\boldsymbol{u} - \boldsymbol{u}_I)$, employing the Bramble-Hilbert lemma would typically require the introduction of the Piola transformation to relate the curl operators $\nabla\times$

and $\hat{\nabla}\times$ within the reference element. However, instead of utilizing the Piola transformation, we introduce the lowest order face element for $H(\mathrm{div};\Omega)$ and leverage a commuting diagram to transition to the estimation of the L^2-error associated with the face element.

1.2. **Face Element.** Given a face f formed by vertices $[i,j,k]$, we introduce a basis vector:

$$\boldsymbol{\phi}_f = 2(\lambda_i\nabla\lambda_j\times\nabla\lambda_k + \lambda_j\nabla\lambda_k\times\nabla\lambda_i + \lambda_k\nabla\lambda_i\times\nabla\lambda_j), \tag{1}$$

and the corresponding degree of freedom:

$$l_f(\boldsymbol{v}) = \int_f \boldsymbol{v}\cdot\boldsymbol{n}\,\mathrm{d}S \approx \boldsymbol{v}(\boldsymbol{c})\cdot\boldsymbol{n}_f|f|, \tag{2}$$

where $\boldsymbol{n}$ is a unit normal vector of f and the quadrature is exact for linear polynomials $\boldsymbol{v}$.

Exercise 1.2. [Face element]

(1) Verify that $\{l_{f_i}, i=1,2,3,4\}$ is a dual basis to $\{\boldsymbol{\phi}_{f_j}, j=1,2,3,4\}$.
(2) For a triangle in 2D, the degree of freedom remains unchanged. Write out the basis functions. A plot of basis for 2D RT element can be found in Fig. 4.

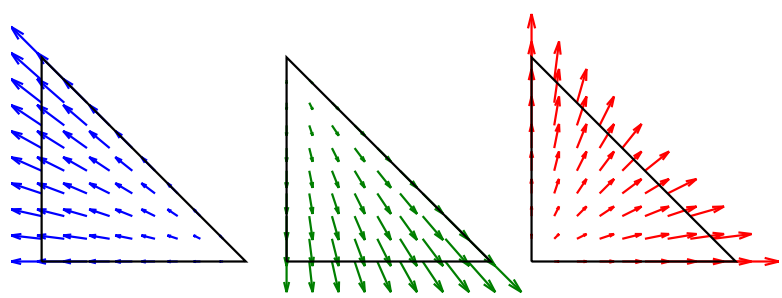

FIGURE 4. Basis vectors $\boldsymbol{\phi}_k$ of RT_0 in a triangle.

We define the lowest order face element space, known as Raviart-Thomas element [7]

$$\mathrm{RT}_0(T) = \mathrm{span}\{\boldsymbol{\phi}_{f_j}, j=1,2,3,4\}$$

and the global version

$$\begin{aligned}\mathrm{RT}_0(\mathcal{T}_h) &= \mathrm{span}\{\boldsymbol{\phi}_f, f\in\mathcal{F}_h\}\\ &= \{\boldsymbol{v}\in L^2(\Omega), \boldsymbol{v}\,|_T\in \mathrm{RT}_0(T), \forall T\in\mathcal{T}_h,\ l_f(\boldsymbol{v}) \text{ is single valued } \forall f\in\mathcal{F}_h\},\end{aligned}$$

where $\mathcal{F}_h$ is the set of all faces of a triangulation $\mathcal{T}_h$.

Given a triangulation $\mathcal{T}_h$ with mesh size h, define $I_h^{\mathrm{div}}: V\to \mathrm{RT}_0(\mathcal{T}_h)$ as follows: for a given function $\boldsymbol{u}\in V$, define $\boldsymbol{u}_I = I_h^{\mathrm{div}}\boldsymbol{u}\in\mathrm{RT}_0(\mathcal{T}_h)$ by matching the degrees of freedom:

$$l_f(I_h^{\mathrm{div}}\boldsymbol{u}) = l_f(\boldsymbol{u}) \quad \forall f\in\mathcal{F}_h(\mathcal{T}_h).$$

That is,

$$\boldsymbol{u}_I = \sum_{f\in\mathcal{F}_h}\left(\int_f \boldsymbol{u}\cdot\boldsymbol{n}\,\mathrm{d}S\right)\boldsymbol{\phi}_f.$$

We verify the crucial commuting property.

Lemma 1.3. *For a function $\boldsymbol{u}\in C^1(\bar{\Omega})$, we have*

$$\nabla\times I_h^{curl}\boldsymbol{u} = I_h^{div}\nabla\times\boldsymbol{u}.$$

Proof. By Stokes' theorem and the definition of interpolation operators:

$$\begin{aligned}\int_f I_h^{\text{div}}(\nabla\times\boldsymbol{u})\cdot\boldsymbol{n}_f\,\mathrm{d}S &= \int_f(\nabla\times\boldsymbol{u})\cdot\boldsymbol{n}_f\,\mathrm{d}S\\ &= \int_{\partial f}\boldsymbol{u}\cdot\boldsymbol{t}\,\mathrm{d}s\\ &= \int_{\partial f} I_h^{\text{curl}}\boldsymbol{u}\cdot\boldsymbol{t}\,\mathrm{d}s\\ &= \int_f(\nabla\times I_h^{\text{curl}}\boldsymbol{u})\cdot\boldsymbol{n}_f\,\mathrm{d}S.\end{aligned}$$

□

Remark 1.4. The domain of the canonical interpolation $I_h^{\text{curl}}, I_h^{\text{div}}$ are smooth subspaces of $H(\text{curl};\Omega)$ or $H(\text{div};\Omega)$, respectively. For instance, even $\boldsymbol{u}\in H^1$, the trace $\boldsymbol{u}$ restricted to an edge may not be well defined. The arguments above necessitate the function to be sufficiently smooth. Quasi-interpolation operators [1, page 65-67], which allow for less stringent smoothness requirements for the function and maintain the desirable commuting diagram, have been developed.

1.3. **Interpolation Error Estimate.** We first prove a stability result for the I_h^{div} operator.

Lemma 1.5. *For $\boldsymbol{v}\in\boldsymbol{H}^1(\Omega)$, we have*

$$\|I_h^{div}\boldsymbol{v}\|\lesssim\|\boldsymbol{v}\|+h\|\nabla\boldsymbol{v}\|.$$

Proof. It suffices to prove the inequality restricted to a single element T. By definition and the Minkowski inequality,

$$\|I_h^{\text{div}}\boldsymbol{v}\|_{0,T}=\|\sum_{f\in\mathcal{F}_h(T)}l_f(\boldsymbol{v})\boldsymbol{\phi}_f\|\le\sum_{f\in\mathcal{F}_h(T)}|l_f(\boldsymbol{v})|\|\boldsymbol{\phi}_f\|_{0,T}.$$

We apply the scaled trace inequality for $w\in H^1(T)$,

$$\|w\|_{0,f}\lesssim h^{-1/2}\|w\|_{0,T}+h^{1/2}\|\nabla w\|_{0,T},$$

and consider the scaling of $\boldsymbol{\phi}_f$ to obtain the desired result. □

We then utilize the commuting diagram to establish the energy error estimate for the I_h^{curl} operator.

Lemma 1.6. *Assume* $\operatorname{curl}\boldsymbol{u}\in\boldsymbol{H}^1(\Omega)$ *and* $\boldsymbol{u}\in Dom(I_h^{curl})$. *Let* $\boldsymbol{u}_I=I_h^{curl}\boldsymbol{u}$. *Then, we have the first-order interpolation error estimate*

$$\|\nabla\times(\boldsymbol{u}-\boldsymbol{u}_I)\|\lesssim h\|\operatorname{curl}\boldsymbol{u}\|_1.$$

Proof. We exploit the commutative property and the fact that I_h^{div} preserves constant vectors to obtain

$$\|\nabla\times(\boldsymbol{u}-\boldsymbol{u}_I)\|=\|(I-I_h^{\text{div}})\nabla\times\boldsymbol{u}\|=\|(I-I_h^{\text{div}})(\nabla\times\boldsymbol{u}-\boldsymbol{c})\|.$$

Subsequently, by the stability of the I_h^{div} operator, we deduce that

$$\|(I-I_h^{\text{div}})(\nabla\times\boldsymbol{u}-\boldsymbol{c})\|\lesssim\|\operatorname{curl}\boldsymbol{u}-\boldsymbol{c}\|+h\|\operatorname{curl}\boldsymbol{u}\|_1.$$

As this holds for any arbitrary constant vector $\boldsymbol{c}$, by selecting $\boldsymbol{c}$ as the average of $\operatorname{curl}\boldsymbol{u}$ and applying the Poincaré inequality, we arrive at the desired error estimate. □

Note that obtaining an L^2-error estimate for the interpolation error of I_h^{curl} is nontrivial and can be accomplished using an inequality for $l_e(\boldsymbol{v})$ on the reference element; see [3, Theorem 3.14].

2. Finite Element Approximation

Let $V = H_0(\text{curl};\Omega)$ and $S = H_0^1(\Omega)$. We consider the saddle-point formulation of Maxwell's equations:

$$(\alpha\nabla\times\boldsymbol{u},\nabla\times\boldsymbol{v}) + (\beta\boldsymbol{v},\nabla p) = (\boldsymbol{f},\boldsymbol{v}) \quad \forall \boldsymbol{v}\in V, \tag{3a}$$

$$(\beta\boldsymbol{u},\nabla q) = 0 \quad \forall q\in S. \tag{3b}$$

Recall that

$$-\langle \text{div}^w(\beta\boldsymbol{u}), q\rangle := (\beta\boldsymbol{u},\nabla q) \quad \forall q\in H_0^1(\Omega),$$

and

$$X = H_0(\text{curl};\Omega)\cap \ker(\text{div}^w).$$

For the inf-sup condition of (3) using the divergence free subspace X, we refer to Variational Formulation of Maxwell's Equations.

For finite element approximation, we choose an edge element space $V_h\subset H_0(\text{curl};\Omega)$ and define the subspace

$$X_h = V_h\cap\ker(\text{div}_h),$$

where $\text{div}_h : V_h\to S_h\subset H_0^1(\Omega)$ is the discrete weak divergence operator, defined as the adjoint of ∇, that is,

$$(\text{div}_h\, v_h, p_h) = (v_h,\nabla p_h) \quad \forall p_h\in S_h.$$

Functions in X_h are referred to as discrete divergence-free, which is not divergence-free. Specifically, X_h is not a subspace of X because the test function space is reduced from S to a subspace S_h.

We can elevate $v_h\in X_h$ to X by using the L^2-projection Q_X. That is, $v = Q_X v_h\in X$ satisfies

$$(v,\xi) = (v_h,\xi) \quad \forall \xi\in X.$$

Since X is a subspace of $L^2(\Omega)$, such an L^2-projection exists and is unique. The subsequent result demonstrates that we can elevate a discrete divergence-free function to a divergence-free one with a controllable difference. In the proof, we require quasi-interpolation operators $\mathcal{I}_h^{\text{d}}$ satisfying properties outlined in Section 3.

Lemma 2.1. *Given $v_h\in X_h$, let $v = Q_X v_h$ be its L^2-projection to X. Then*

(1) $\text{curl}\, v = \text{curl}\, v_h$;

(2) $\|v\| \eqsim \|v_h\|$;

(3) $\|v - v_h\| \lesssim h^s \|\text{curl}\, v_h\|$.

Proof. We solve a Poisson equation to find $p\in H_0^1(\Omega)$ such that

$$(\nabla p,\nabla\phi) = -(v_h,\nabla\phi) \quad \forall\phi\in H_0^1(\Omega).$$

Let us define v as

$$v = v_h + \nabla p.$$

It is straightforward to demonstrate that $v = Q_X v_h$ by verifying the orthogonality to $\nabla H_0^1(\Omega)$:

$$(v - v_h,\nabla\phi_h) = (\nabla p,\nabla\phi_h) = -(v_h,\nabla\phi_h) = 0 \quad \forall\phi_h\in S_h. \tag{4}$$

The result (1) is trivial since $\text{curl}\,(\nabla p) = 0$.

(2) By the definition of L^2-projection, $\|v\| \leq \|v_h\|$. We need to control $\|v - v_h\|$. Initially, we assert that $\nabla \times (\mathcal{I}_h^{\text{curl}} v - v_h) = 0$ as

$$\nabla \times \mathcal{I}_h^{\text{curl}} v = \mathcal{I}_h^{\text{div}}(\nabla \times v) = \mathcal{I}_h^{\text{div}}(\nabla \times v_h) = \nabla \times v_h.$$

Then, by the exactness of the finite element de Rham complex, there exists $\phi_h \in S_h$ such that $\mathcal{I}_h^{\text{curl}} v - v_h = \nabla \phi_h$.

Utilizing the orthogonality from equation (4),

$$(v - v_h, v - v_h) = (v - v_h, v - \mathcal{I}_h^{\text{curl}} v) + (v - v_h, \mathcal{I}_h^{\text{curl}} v - v_h) = (v - v_h, v - \mathcal{I}_h^{\text{curl}} v),$$

which implies

$$\|v - v_h\| \leq \|v - \mathcal{I}_h^{\text{curl}} v\| \lesssim \|v\|.$$

(3) We use the embedding result $\|v\|_s \lesssim \|\text{curl}\, v\|, v \in X$, for some $s \in (1/2, 1]$ and the interpolation error estimate of $\mathcal{I}_h^{\text{curl}}$

$$\|v - v_h\| \leq \|v - \mathcal{I}_h^{\text{curl}}\, v\| \lesssim h^s \|v\|_s \lesssim h^s \|\text{curl}\, v\| = h^s \|\text{curl}\, v_h\|.$$

□

Recall that we have the following Poincaré inequality (Lemma 4.3) Variational Formulation of Maxwell's Equations:

$$\|\boldsymbol{v}\| \lesssim \|\text{curl}\, \boldsymbol{v}\| \quad \text{for } \boldsymbol{v} \in X. \tag{5}$$

We will establish the following discrete Poincaré inequality on X_h. It is not a simple consequence of the Poincaré inequality (5) as $X_h \not\subset X$.

Lemma 2.2 (Discrete Poincaré Inequality)**.** *When Ω is topologically trivial and $\mathcal{T}_h$ is shape regular, then*

$$\|v_h\| \lesssim \|\text{curl}\, v_h\| \quad \textit{for } v_h \in X_h.$$

Proof. We elevate v_h to X, that is, $v = Q_X v_h$, and apply the Poincaré inequality to v. The desired discrete version is derived from the properties of v in Lemma 2.1:

$$\|v_h\| \lesssim \|v\| \lesssim \|\text{curl}\, v\| = \|\text{curl}\, v_h\|.$$

□

Now, let us consider the finite element discretization of the saddle point formulation: find $\boldsymbol{u}_h \in V_h, p_h \in S_h$ such that

$$(\alpha \nabla \times \boldsymbol{u}_h, \nabla \times \boldsymbol{v}_h) + (\beta \boldsymbol{v}_h, \nabla p_h) = (\boldsymbol{f}, \boldsymbol{v}_h) \quad \forall \boldsymbol{v}_h \in V_h, \tag{6}$$

$$(\beta \boldsymbol{u}_h, \nabla q_h) = 0 \quad \forall q_h \in S_h. \tag{7}$$

The discrete inf-sup condition for div_h is straightforward because its adjoint $\nabla : S_h \to V_h$ is injective. The coercivity in $\ker(\text{div}_h)$ is guaranteed by the discrete Poincaré inequality. Consequently, the well-posedness of equations (6)-(7) is derived from Brezzi's theory, and we obtain the first-order error estimate. We summarize this in the following theorem.

Theorem 2.3. *There exists a unique solution $(\boldsymbol{u}_h, p_h)$ to (6)-(7). When $\text{curl}\, u \in H^1(\Omega)$ and $p \in H^2(\Omega)$, we have*

$$\|\alpha^{1/2} \nabla \times (\boldsymbol{u} - \boldsymbol{u}_h)\| + \|\beta^{1/2} \nabla (p - p_h)\| \lesssim h \left(\|\nabla \times \boldsymbol{u}\|_1 + \|p\|_2 \right).$$

When $\text{div}\, \boldsymbol{f} = 0$, we have both $p = p_h = 0$ and

$$\|\alpha^{1/2} \nabla \times (\boldsymbol{u} - \boldsymbol{u}_h)\| \lesssim h \|\nabla \times \boldsymbol{u}\|_1.$$

Proof. By Brezzi theory and interpolation error estimate, we have

$$\begin{aligned}\|\alpha^{1/2}\nabla\times(\boldsymbol{u}-\boldsymbol{u}_h)\|+\|\beta^{1/2}\nabla(p-p_h)\| &\lesssim \|\nabla\times(\boldsymbol{u}-\boldsymbol{u}_I)\|+\|\nabla(p-p_I)\| \\ &\lesssim h\left(\|\nabla\times\boldsymbol{u}\|_1+\|p\|_2\right).\end{aligned}$$

When $\operatorname{div}\boldsymbol{f}=0$, we have both $p=p_h=0$. □

The symmetric formulation

$$\nabla\times(\alpha\nabla\times\boldsymbol{u})+\beta\boldsymbol{u}=\boldsymbol{f}\quad\text{in }\Omega,\qquad \boldsymbol{u}\times\boldsymbol{n}=0\quad\text{on }\partial\Omega \tag{8}$$

is simpler and leave as an exercise.

3. DE RHAM COMPLEX AND FINITE ELEMENT DE RHAM COMPLEX

We compile the sequence and the interpolation operators to form the following diagram:

$$\begin{tikzcd}
\mathbb{R} \arrow[r, "\subset"] & H^1(\Omega) \arrow[r, "\mathrm{grad}"] \arrow[d, "\mathcal{I}_h^{\mathrm{grad}}"] & H(\mathrm{curl};\Omega) \arrow[r, "\mathrm{curl}"] \arrow[d, "\mathcal{I}_h^{\mathrm{curl}}"] & H(\mathrm{div};\Omega) \arrow[r, "\mathrm{div}"] \arrow[d, "\mathcal{I}_h^{\mathrm{div}}"] & L^2(\Omega) \arrow[r] \arrow[d, "\mathcal{I}_h^{L^2}"] & 0 \\
\mathbb{R} \arrow[r, "\subset"] & S_h \arrow[r, "\mathrm{grad}"] & V_h \arrow[r, "\mathrm{curl}"] & U_h \arrow[r, "\mathrm{div}"] & Q_h \arrow[r] & 0
\end{tikzcd}, \tag{9}$$

where S_h is the standard linear finite element space, V_h is the lowest-order edge element space, U_h is the lowest-order face element space, and Q_h is the piecewise constant space.

In the diagram, the interpolation operators are not the canonical interpolation operators, which are not well-defined for $H(\mathrm{d};\Omega)$ spaces. We assume the existence of quasi-interpolation operators $\mathcal{I}_h^{\mathrm{d}}$ with the following properties:

- $\mathrm{dom}(\mathcal{I}_h^{\mathrm{d}})\subseteq H(\mathrm{d};\Omega)$;
- L^2-stable: $\|\mathcal{I}_h^{\mathrm{d}}v\|\lesssim\|v\|$;
- projection: $\mathcal{I}_h^{\mathrm{d}}v=v$ if v is in finite element space;
- commutative with differential operators $\mathrm{d}\,\mathcal{I}_h^{\mathrm{d}-}=\mathcal{I}_h^{\mathrm{d}}\,\mathrm{d}$.

Such operators can be found in [1, page 65-67] and [2].

Exercise 3.1. Prove the commuting diagram

$$\mathrm{d}\,I_h^{\mathrm{d}-}=I_h^{\mathrm{d}}\,\mathrm{d}$$

when the quasi-interpolation operators $\mathcal{I}_h^{\mathrm{d}}$ are replaced by the following cannoical interpolation operators I_h^{d}:

$$I_h^{\mathrm{grad}}v(x_i)=v(x_i),\qquad \int_e I_h^{\mathrm{curl}}\boldsymbol{u}\cdot\boldsymbol{t}\,\mathrm{d}s=\int_e\boldsymbol{u}\cdot\boldsymbol{t}\,\mathrm{d}s$$

$$\int_f I_h^{\mathrm{div}}\boldsymbol{u}\cdot\boldsymbol{n}\,\mathrm{d}S=\int_f\boldsymbol{u}\cdot\boldsymbol{n}\,\mathrm{d}S,\qquad \int_T I_h^{L^2}v\,\mathrm{d}x=\int_T v\,\mathrm{d}x.\qquad\square$$

The top sequence in diagram (9) is recognized as a Hilbert complex, specifically known as the de Rham complex. This complex satisfies the properties: $\mathrm{curl}\,\mathrm{grad}=0$, $\mathrm{div}\,\mathrm{curl}=0$, and each operator within the sequence has a closed range. The closed range of each operator implies the existence of a corresponding Poincaré inequality. The sequence is deemed exact if it fulfills the condition $\ker(\mathrm{d})=\mathrm{img}(\mathrm{d}^-)$, where d^- denotes the operator preceding d in the sequence. When the domain Ω exhibits trivial topology, meaning it is simply connected and its boundary is also connected, one can confirm that the top sequence is indeed exact.

In a more general context, the quotient space $\ker(\mathrm{d}_{k+1})/\mathrm{img}(\mathrm{d}_k)$ is defined as the k-th cohomology space of Ω. These cohomology spaces are finite-dimensional vector spaces, and their dimensions are identified by the Betti numbers β_k of the manifold Ω. For a bounded connected region in $\mathbb{R}^3$, the Betti numbers are characterized as follows: $\beta_0 = 1$ corresponds to the number of connected components, β_1 represents the genus (or the number of handles), β_2 denotes the number of connected components of the boundary (or the number of holes), and $\beta_3 = 0$ for a three-dimensional region.

We provide further clarification on the concept of exactness. Consider a vector field u such that $\operatorname{curl} u = 0$ within a connected domain Ω. Our goal is to identify a scalar potential function p satisfying $u = \operatorname{grad} p$. The approach involves utilizing the line integral along a curve C that connects a fixed point x_0 to a variable point x, expressed as $p(x) = \int_{C[x_0,x]} u(s) \cdot \mathrm{d}s$. Subsequently, it can be readily confirmed that $u = \operatorname{grad} p$. A classic illustration of this is the gravitational field.

For p to be well-defined, the line integral must be invariant with respect to the path chosen. If two curves C_1 and C_2 share the same endpoints, they delineate the boundary of a two-dimensional surface S. Given $\operatorname{curl} u = 0$, Stokes' theorem can be invoked to deduce that

$$\int_S \operatorname{curl} u \cdot \mathrm{d}S = \int_{\partial S} u \cdot \mathrm{d}s = \int_{C_1} u \cdot \mathrm{d}s - \int_{C_2} u \cdot \mathrm{d}s = 0.$$

The negative sign arises from the consideration of orientation. A topological restriction arises from the fact that not every closed curve is the boundary of a closed surface, such as a curve that encircles a hole.

For a divergence-free vector field u, determining its vector potential ϕ is a more complex task. Specifically, given $\operatorname{div} u = 0$, we seek a vector field ϕ such that $u = \operatorname{curl} \phi$. We will omit the detailed process here but note that the existence of such a potential is contingent upon the topology of the domain. A relevant physical example is the electric field created by a charge located at the origin, given by

$$u(x, y, z) = \frac{(x, y, z)}{(x^2 + y^2 + z^2)^{3/2}}.$$

In this case, $\operatorname{div} u = 0$ everywhere except at the origin. However, u cannot be expressed as $\operatorname{curl} \phi$ because $\int_S u \cdot n \, \mathrm{d}S = 4\pi$ for any closed and positively oriented surface S that encloses the origin.

Utilizing the commuting property, we can confirm that the bottom sequence in the diagram will preserve the cohomology, a property that characterizes the finite element de Rham complex. In particular, when the domain Ω has the trivial topology, the finite element de Rham complex is also exact. Given a function $v_h \in V_h$ with $\operatorname{curl} v_h = 0$, and since $V_h \subset H(\operatorname{curl}; \Omega)$, we can identify a potential $p \in H^1(\Omega)$ such that $v_h = \operatorname{grad} p$. The scalar function p may not be within the finite element space. We define $p_h = \mathcal{I}_h^{\mathrm{grad}} p$ and apply the commuting diagram to deduce that

$$\operatorname{grad} \mathcal{I}_h^{\mathrm{grad}} p = \mathcal{I}_h^{\mathrm{curl}} \operatorname{grad} p = \mathcal{I}_h^{\mathrm{curl}} v_h = v_h.$$

The verification of the other blocks in the diagram can be carried out in a similar manner. Adapting the space to include functions with zero trace is also a straightforward process.

A systematic approach to studying finite element methods through the lens of differential forms is recognized as FEEC (finite element exterior calculus). In this context, we provide only an introductory overview and direct the reader to the comprehensive survey by Arnold, Falk, and Winther [1] for a detailed understanding of the general framework.

For insights into the more specific application of these methods to the field of electromagnetism, we refer to the work of Hiptmair [3].

ACKNOWLEDGMENTS

We express our gratitude to Dr. Shuhao Cao for his enlightening discussions and for his assistance in creating the illustrative figures of basis functions. We also extend our thanks to Dr. Yongke Wu for his contributions to the proof of the discrete Poincaré inequality.

REFERENCES

[1] D. N. Arnold, R. S. Falk, and R. Winther. Finite element exterior calculus, homological techniques, and applications. *Acta Numer.*, pages 1–155, 2006. 5, 8, 9

[2] S. H. Christiansen and R. Winther. Smoothed projections in finite element exterior calculus. *Math. Comp.*, 77(262):813, 2008. 8

[3] R. Hiptmair. Finite elements in computational electromagnetism. *Acta Numer.*, pages 237–339, 2002. 6, 10

[4] P. Monk. *Finite Element Methods for Maxwell's Equations*. Oxford University Press, 2003.

[5] J. Nédélec. Mixed finite elements in R^3. *Numer. Math.*, 35:315–341, 1980. 1

[6] J. Nédélec. A new family of mixed finite elements in R^3. *Numer. Math.*, 50:57–81, 1986. 1

[7] P. A. Raviart and J. Thomas. A mixed finite element method fo 2-nd order elliptic problems. In I. Galligani and E. Magenes, editors, *Mathematical aspects of the Finite Elements Method*, Lectures Notes in Math. 606, pages 292–315. Springer, Berlin, 1977. 4